Spectrochimica Acta Part A: Molecular and Biomolecular Spectroscopy 334 (2025) 125928

Contents lists available at ScienceDirect

Spectrochimica Acta Part A: Molecular and Biomolecular Spectroscopy

journal homepage: www.journals.elsevier.com/spectrochimica-acta-part-a-molecular-and-biomolecular-spectroscopy

Chitin and chitosan quantification in fungal cell wall via Raman spectroscopy

Suset Barroso-Solares [a,b,*], Federico Lopez-Moya [c], Teresa Fraile [c], Ángel Carmelo Prieto [a], Luis Lopez-Llorca [c], Javier Pinto [a,b,*]

[a] Study, Preservation, and Recovery of Archaeological, Historical and Environmental Heritage (AHMat) Research Group, Condensed Matter Physics, Crystallography, and Mineralogy Department, Faculty of Science, University of Valladolid 47011 Valladolid, Spain
[b] BioEcoUVA Research Institute on Bioeconomy, University of Valladolid, Spain
[c] Department of Marine Sciences and Applied Biology, Laboratory of Plant Pathology, University of Alicante 03690 Alicante, Spain

HIGHLIGHTS

- A new approach for the study of chitosan in fungi strains is proposed.
- Raman spectroscopy allows determining the relative chitosan content in fungi.
- Combining this approach with acid hydrolysis can provide absolute values.

GRAPHICAL ABSTRACT

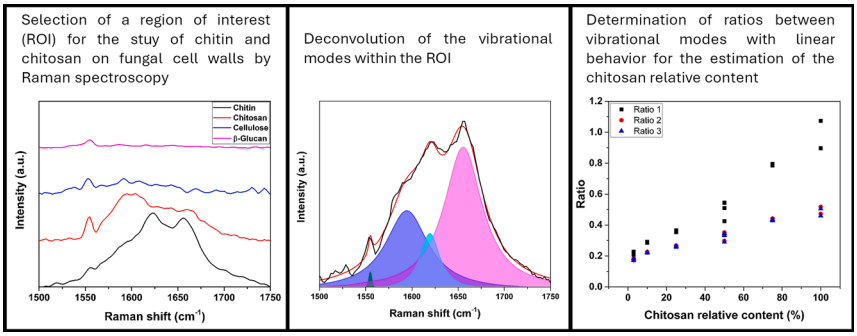

ARTICLE INFO

Keywords:
Biocontrol fungi
Chitin
Chitosan
Aminopolysaccharides
Raman spectroscopy

ABSTRACT

Investigation of cell wall composition is necessary to understand the interactions between fungi and the environment as it is the external layer exposed to stimuli and detected by other organisms. *Pochonia chlamydosporia* and *Akanthomyces lecanii*, two fungal species living in the soil and infecting nematodes and insects, exhibit endophytic interactions with various plant species. Determination of cell wall composition is essential to understand the mechanisms underlying these interactions. Therefore, in this study, for the first time, we assessed the relative amounts of chitin and chitosan in the cell walls of *P. chlamydosporia* (PC123) and *A. lecanii* (69NZ, 85SCT, 126KNY, and 447SAF) via Raman spectroscopy. The isolate with the highest chitosan percentage was 69NZ, followed by 85SCT, PC123, 447SAF, and 126KNY. Moreover, combination with conventional approaches for chitin and chitosan quantification yielded quantitative results for all cell wall components. Overall, these results highlight the mechanisms by which fungi exhibit chitosan resistance and avoid detection by the host plant during root colonization.

* Corresponding authors at: Study, Preservation, and Recovery of Archaeological, Historical and Environmental Heritage (AHMat) Research Group, Condensed Matter Physics, Crystallography, and Mineralogy Department, Faculty of Science, University of Valladolid, 47011 Valladolid, Spain.
E-mail addresses: suset.barroso@uva.es (S. Barroso-Solares), javier.pinto@uva.es (J. Pinto).

https://doi.org/10.1016/j.saa.2025.125928
Received 12 September 2024; Received in revised form 26 December 2024; Accepted 17 February 2025
Available online 18 February 2025

1. Introduction

Recently, Raman spectroscopy has attracted significant interest for study of biomolecules. It exhibits high sensitivity for chemistry and structure analyses and provides specific Raman signatures for different cellular components, facilitating the identification of diverse compounds in biological samples [1,2]. Moreover, Raman spectroscopy is non-destructive, highly sensitive, and does not require prior sample preparation [3–5].

Reliable and accurate determination of fungal cell wall composition remains a challenge in fungal biology and ecology despite its crucial impacts on cell shape, viability, and interactions with the environment. Both common components and specialized molecules specific to each species are important to define fungal ecology [6]. Fungal cell wall is the key target of important antifungals, such as echinocandins [7].

Spectroscopic techniques are useful to assess the cell wall composition and biological structure. Raman spectroscopy in the microscopic mode has been used to detect chitin in the skeleton of the marine sponge, *Aplysina fistularis* [2]. This technique can differentiate α-chitin, β-chitin, and γ-chitin due to noticeable differences in their amide I vibration bands [8]. Moreover, Raman spectroscopy is sensitive to substitutions in the structure of glucans, degree of crystallinity of compounds, such as cellulose, and various impurities [9,10]. It is an accurate technique to determine the degree of N-acetylation in chitosan [11]. It has been used to estimate the relative contents of starch and β-glucan in barley and oat samples [12].

Recent studies have focused on chitin and chitosan components in the fungal cell wall [13,14]. These aminopolysaccharides are among the most abundant natural biopolymers that are widely distributed in the biosphere. Owing to their unique physicochemical properties, they exhibit remarkable biological activities and are beneficial for the chemical, healthcare, food, and agricultural industries [13]. Chitosan shows antimicrobial activities against plant pathogenic fungi and bacteria. It is also described as plant defense inducer, mainly inducing jasmonic and salicylic acids (JA and SA) phytohormones. Chitosan also is a compatible compound with biocontrol agents, mainly nematophagous and entomopathogenic fungi. Chitin is converted into chitosan by various chitin deacetylases [15], which are important for various fungal pathogens and mutualists to avoid host immune responses [16]. For example, nematophagous fungi can convert their and the host chitin into chitosan using chitin deacetylases to avoid plant defenses during infection of nematodes eggs in plant tissues [17].

Raman spectroscopy is used to detect chitin and determine the degree of N-acetylation in chitosan [2,11,14]. However, key parameters, such as the chitosan:chitin ratio, have not been assessed using this technique. Standard chemical techniques, such as acid hydrolysis, used for the study of fungal cell wall composition only provide the total chitin and chitosan contents owing to the detachment of acetyl groups on chitin monomers, thereby increasing the difficulty of distinguishing between the two molecules [18]. More complex extraction approaches based on non-soluble materials at alkaline pH have been developed to determine the chitosan concentration in the fungal cell wall [19–21], which is commonly expressed as chitosan yield.

In this study, we aimed to develop a new methodology based on Raman spectroscopy to determine the chitosan:chitin mass ratio in the fungal cell wall. Additionally, we combined the developed approach with conventional acid hydrolysis technique to determine the concentration of each component in the fungal cell wall.

2. Materials and methods

2.1. Sample preparation

Strains of the nematophagous fungus, *Pochonia chlamydosporia* (PC123), and entomopathogenic fungus, *Akanthomyces lecanii* (69NZ, 85SCT, 126KNY, and 447SAF), were obtained from the Plant Pathology Laboratory of University of Alicante (Spain). PC123 was isolated from *Heterodera avenae* eggs in southwest Spain [22]. Strains 69NZ, 85SCT, 126KNY, and 447SAF from New Zealand, Scotland, Kenya, and South Africa, respectively, were kindly provided by Professor Brian Kerry (Rothamsted Research, Harpenden, UK).

P. chlamydosporia is a nematophagous fungus that lives in the soil and colonizes plant roots. Its nematophagous behavior is mainly based on its ability to parasitize the nematode egg shell, which is largely composed of chitin [22]. Owing to its ability to colonize nematode eggs, *P. chlamydosporia* is widely used as a biological control agent for the management of nematode pests in agriculture [23]. *A. lecanii* is an entomopathogenic fungus with various hosts that acts as an endophyte in some economically relevant crops [24,25]. This fungus can also infect nematode eggs [26]. These microbes must degrade chitin rich egg-shell/cuticle of their hosts upon their infection. As fungal chitin induces plant defense responses, it threatens the survival of both species in the rhizosphere [27,28]. Chitin deacetylation generates chitosan and reduces changes of fungal detection by plants.

Notably, both fungi exhibit chitosan resistance, possibly due to their cell wall composition. Aranda-Martinez *et al.* investigated the cell wall composition of *Neurospora Crassa*, a species sensitive to chitosan and that of the chitosan resistant fungus *P. chlamydosporia* [29]. Their study indicate that an increase in β-1,3-glucan/chitin ratio favors fungal resistance to chitosan [30].

Conidia of the selected fungi (final concentration: 10^6 conidia/mL) were inoculated into a 250 mL flask with 50 mL of Czapek Doz medium, as previously described [26]. The flasks were incubated at 25 °C with shaking at 120 rpm. After seven days, the mycelia were recovered via filtration through the Miracloth (Calbiochem. San Diego, CA, USA), washed with sterile distilled water, and lyophilized. Fungal tissue were frozen in liquid nitrogen and homogenized using a mortar and pestle. Commercial samples of the key pure components of cell walls, namely cellulose (Sigma-Aldrich, St. Louis, MO, USA), β-glucan (USP, Rockville, MD, USA), chitosan (Marine Bioproducts GmbH, Bremerhaven, Germany), and chitin (Sigma- Aldrich), were also lyophilized and milled prior to use.

2.2. Chemical characterization

Chitin and chitosan contents of the mycelia were estimated by determining the amounts of N-acetylglucosamine and glucosamine, as previously described [29]. Briefly, the fungal samples (30 mg) were hydrolyzed in 1 mL of 6 N HCl at 110 °C for 6 h. HCl was air dried in a fume hood, and samples were resuspended in 1 mL of sterile distilled water and centrifuged twice at 24,681 × *g* for 20 min each. Then, 0.5 mL aliquot of the supernatant from each sample was mixed with 0.1 mL of 0.16 M sodium tetraborate (pH 9.1) and heated at 100 °C for 3 min. After cooling, 3 mL of p-dimethylamine benzaldehyde solution (10 % dimethylamine benzaldehyde in glacial acetic acid containing 12.5 % HCl [10 N] diluted with 9 vol of glacial acetic acid) was added. The mixture was incubated for 20 min at 37 °C and absorbance at 595 nm was measured using the Genios Multiwell Spectrophotometer (Tecan, Männedorf, canton of Zürich, Switzerland). A standard curve was plotted using 0–40 mg/mL N-acetyl-D-glucosamine (Sigma-Aldrich) also hydrolyzed as described above. This procedure was repeated twice to obtain 54 replicates for each isolate. This method facilitated the quantification of the total amounts of chitin and chitosan in a given sample, as previously described [18].

2.3. Raman spectroscopy

A portable BWTEK Raman spectrometer equipped with the BTWTEK Exemplar Pro (CCD BTC675N) (B&W Tek, Plainsboro, NJ, USA) detector was used in macroscopic mode (spot size: approximately 85 μm) to ensure a measurement area representative of the fungal cell wall composition. The λ = 785 nm line from a diode laser was used as the

exciting beam. The nominal laser power for the sample was approximately 186 mW, with an approximate irradiance of 820 W·cm^2. The acquisition time was 100–180 s with three accumulations. All spectra were recorded in the range of 100–3200 cm^{-1}, with a spectral resolution of 4.5 cm^{-1}. Prior to Raman measurements, most samples were photobleached for about five hours using the same wavelength and irradiance to reduce background fluorescence, particularly that observed due to high chitin content in the fungal cell walls. The remaining fluorescence was removed from the Raman spectra by subtracting the baseline values using Spectragryph software 1.2.12. This software was also employed to determine the maximum peak and center of gravity positions of the broad convoluted Raman bands of the region of interest (i.e., 1500–1750 cm^{-1}, as will be later discussed). Finally, Raman bands within that range were deconvoluted according to the dynamic vibrational Raman modes of chitosan and chitin (Table 1). The fitting process was performed with Origin 2016 software (OriginLab Co., Northampton, MA, USA) using Lorentzian peaks until reaching χ^2 values $<10^{-6}$.

Lyophilized fungal samples, pure cell wall polymers, pure chitosan and chitin, and chitosan and chitin mixtures (3:97, 10:90, 20:80, 25:75, 50:50, and 75:25 [wt%:wt%]) were prepared for Raman spectroscopy. All materials were frozen in liquid nitrogen and milled with an agate mortar to obtain fine powders of small particles and homogenous mixtures. Generally, chitin and chitosan contents in ascomycetes (Table 1), similar to those analyzed in this study, are within the 0–25 wt% range. Reference samples were employed to develop several calibration approaches in order to evaluate the relative chitosan content of actual fungal samples. For the successful calibration approaches, the limit of detection (LOD) was estimated as LOD = 3 SD(intercept)/S, where SD is the standard deviation of the intercept and S is the slope.

3. Results and discussion

In this study, chitin and chitosan contents varied among the tested fungal strains (Table 2). Strains 126KNY and 69NZ contained higher chitin and chitosan contents than PC123, 85SCT, and 447SAF. Notably, 447SAF strain exhibited the lowest chitin and chitosan contents, with an average of 0.3946 mg/mg of dry mycelium. Conversely, strain 69NZ exhibited the highest chitin and chitosan contents, with an average of 0.5530 mg/mg of dry mycelium weight.

Colorimetric analysis of acid hydrolysates accurately reveals the total chitin and chitosan amounts in fungal samples; however, it cannot determine the relative amounts of each cell wall components [17].

To develop a better approach, we obtained and compared the Raman spectra of a few selected pure components of the cell wall (cellulose, β-glucan, chitosan, and chitin) to identify potential regions of interest for the quantification of chitosan and chitin (Fig. 1a). Consistent with their chemical structures, only chitosan and chitin showed notably Raman bands in the region of interest (1500–1750 cm^{-1}; Fig. 1b). These Raman bands corresponded to the vibrational modes of amide and NH_2 functional groups (Table 3), which are absent in both cellulose and β-glucan. Moreover, chitosan and chitin exhibited characteristic features in the region of interest (Fig. 1b; Table 3). These results indicated the presence of NH_2 groups in chitosan as well as the dynamic relative intensity of the vibrational modes corresponding to amide groups δ(NH) and ν(CO) present lower relative intensities (Table 3). Chitin spectra also exhibited an almost negligible signal at 1555 cm^{-1}, possibly corresponding to ν(CN) [33].

These results indicate that analysis of Raman bands in the 1500–1750 cm^{-1} region can provide information on the relative levels of chitosan and chitin in the fungal cell wall, with no influence of other cell wall polymers, such as cellulose and β-glucan. Therefore, Raman spectra of the experimental mixtures of pure compounds were assessed (Fig. 2).

Clear progressive evolution of the Raman band is directly associated with the relative abundance of chitosan (Fig. 2). To quantify this relationship, peak position and center of gravity of the bands in the 1540–1740 cm^{-1} range were calculated. As shown in Fig. 3, specific trends were observed for both the features and relative contents of chitosan in pure chitosan and chitosan:chitin blends. In contrast, the values corresponding to pure chitin did not follow any specific trend, indicating the dominant Raman response of chitosan in chitosan:chitin blends.

In the chitosan:chitin blends, the maximum value was approximately 1656 cm^{-1} (ν(CO), indicating medium and weak intensities for chitin and chitosan, respectively) until the relative content of chitosan reached approximately 50 wt%, after which it shifted to the 1595–1600 cm^{-1} range (δ(NH_2), indicating medium intensity for chitosan). Regarding the evolution of the center of gravity, a linear trend was observed, facilitating the estimation of the relative chitosan content. However, the range of measurement, approximately 20 cm^{-1} for 3–100 % chitosan content, was narrow considering the spectral resolution of the experimental setup (about 4.5 cm^{-1}). Therefore, this method cannot accurately distinguish small differences in the relative chitosan content using the proposed experimental setup. Nevertheless, Raman spectrometers with high spectral resolutions can aid in the determination of the relative chitosan content in fungal samples using the center of gravity.

Next, Raman spectra were deconvoluted to determine the

Table 1
Chitin and chitosan contents in ascomycete fungi. Fungi closely related to those analyzed in this study are indicated in bold.

Chitosan yield (%)	Fungi	Chitosan/Chitosan + chitin (%)	Ref
	Ascomycetes		
11.0	*Aspergillus niger*	61.11	[31]
3.6	*Zygosaccharomyces rouxii*	33.96	
4.4	*Candida albicans*	38.60	
4.75	*Penicillium chrysogenum*	40.43	[32]
0.3	*Ashbya gossypii*	4.11	[20]
0.9	*Aspergillus clavatus*	11.39	
2.0	*Aspergillus flavus*	22.22	
3.9	*Aspergillus nidulans*	35.78	
0.8	*Aspergillus niger*	10.26	
1.1	*Aspergillus oryzae*	13.58	
0.5	*Aspergillus terreus*	6.67	
3.4	*Aspergillus terricola*	32.69	
1.3	*Aspergillus usamii*	15.66	
1.9	*Botrytis cinerea*	21.35	
2.4	*Ceratocystis* sp.	25.53	
1.99	*Cladosporium cucumerinum*	22.14	
4.1	*Cladosporium cladosporioides*	36.94	
0.7	*Epicoccum nigrum*	9.09	
1.6	*Gliocladium catenulatum*	18.60	
1.0	*Humicola grisea*	12.50	
1.3	***Myrothecium verrucaria***	**15.66**	
0.4	*Penicillium chrysogenum*	5.41	
2.9	*Penicillium digitatum*	29.29	
0.9	***Trichoderma viride***	**11.39**	
0.9	***Trichoderma roseum***	**11.39**	

Table 2
Chitin and chitosan contents of the fungal strains analyzed in this study.

Fungal strain	Chitosan + chitin (mg/mg DW)
69NZ	0.55 ± 0.20
85SCT	0.49 ± 0.28
PC123	0.43 ± 0.22
126KNY	0.55 ± 0.19
447SAF	0.39 ± 0.17

Values are represented as the mean (n = 3) with standard error. No significant differences were observed among the groups (P < 0.05). Abbreviation: DW, mycelium dry weight.

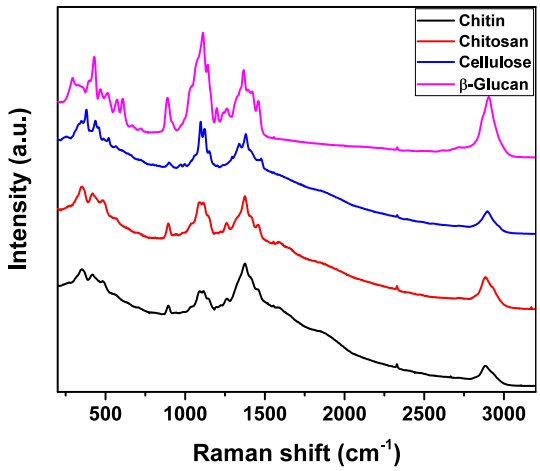

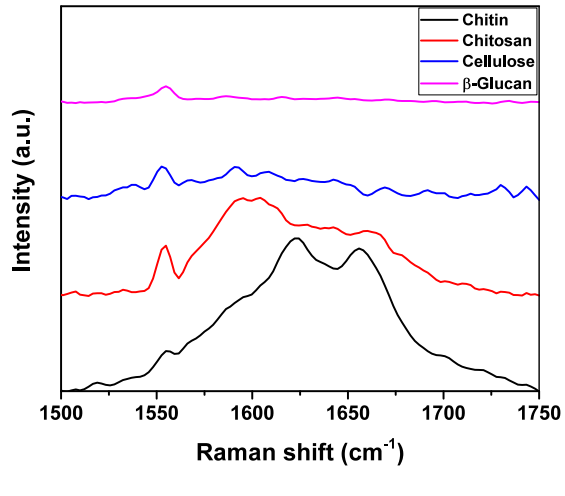

Fig. 1. Raman spectra of chitin, chitosan, cellulose, and β-glucan in the full range (a) and after baseline correction in the region of interest (b).

Table 3
Raman shifts in the bands of chitin and chitosan Raman spectra in the range of interest (1500–1750 cm^{-1}) and their corresponding normal vibrations. Relative Raman intensity of each band is indicated as m (medium) or w (weak), as previously described [11,33].

Chitin		Chitosan	
Raman shift (cm^{-1})	Vibrational mode	Raman shift (cm^{-1})	Vibrational mode
1555w	ν(CN)	1555w	δ(NH_2), ν(CN)
		1595m	δ(NH_2)
1620m	δ(NH)	1620w	δ(NH)
1656m	ν(CO)	1656w	ν(CO)

contribution of each vibrational mode. Based on previous results, only the samples containing chitosan were analyzed. Raman bands of pure chitosan and chitosan:chitin blends in the region of interest (1500–1750 cm^{-1}) were deconvoluted by fitting them to the dynamic vibrational Raman modes of chitosan and chitin. An example of the fitting result is shown in Fig. 4.

From the obtained values, three ratios were used to estimate the relative chitosan content. The first ratio (Ratio 1) related the integrated areas corresponding to δ(NH_2) vibrational modes at 1555 and 1595 cm^{-1} with those of δ(NH) and ν(CO). The second ratio (Ratio 2) related

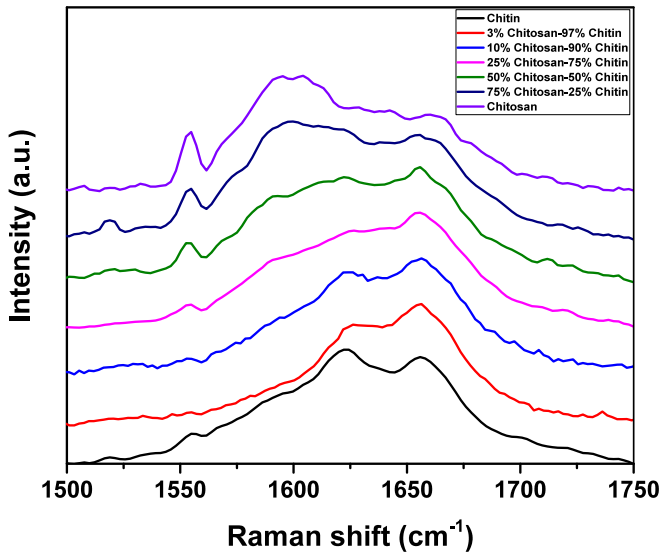

Fig. 2. Raman spectra of pure chitin and chitosan and five blends in the 1500–1750 cm^{-1} range.

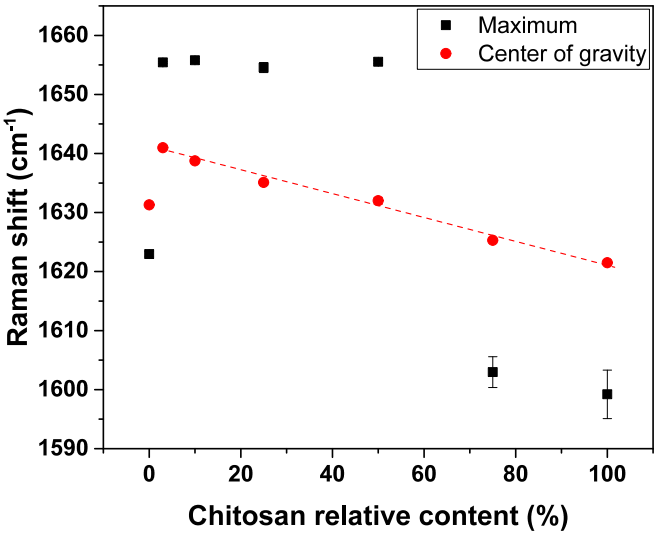

Fig. 3. Change in the maximum and center of gravity of pure chitin and chitosan and chitosan:chitin blend bands in the 1540–1740 cm^{-1} range. Dotted red line indicates the linear trend shown by the center of gravity in the chitosan-containing samples.

the same integrated areas corresponding to δ(NH_2) vibrational modes at 1555 and 1595 cm^{-1} with the total integrated area corresponding to all vibrational modes. The last ratio (Ratio 3) related the integrated area corresponding to δ(NH_2) vibrational mode at 1595 cm^{-1} with the integrated areas corresponding to that and δ(NH) and ν(CO) vibrational modes. Specifically, ratio 3 was used to evaluate the potential influences of other compounds on the 1555 cm^{-1} band (Fig. 1b).

Results are shown in Fig. 5. In all cases, the values provided by these ratios for different samples were linearly fitted (Table 4), achieving calibration equations relating the Raman spectra and relative chitosan contents with R^2 of ca. 0.96–0.97.

The results indicated that any ratio could be used to estimate the relative contents of chitosan and chitin in the fungal cell wall. Moreover, same trends were observed irrespective of the δ(NH_2) band at 1555 cm^{-1}, indicating no significative influence of other compounds in the selected spectral region (1500–1750 cm^{-1}). Estimated LOD provided quite low values, about 0.2–0.4 % of chitosan relative content. This

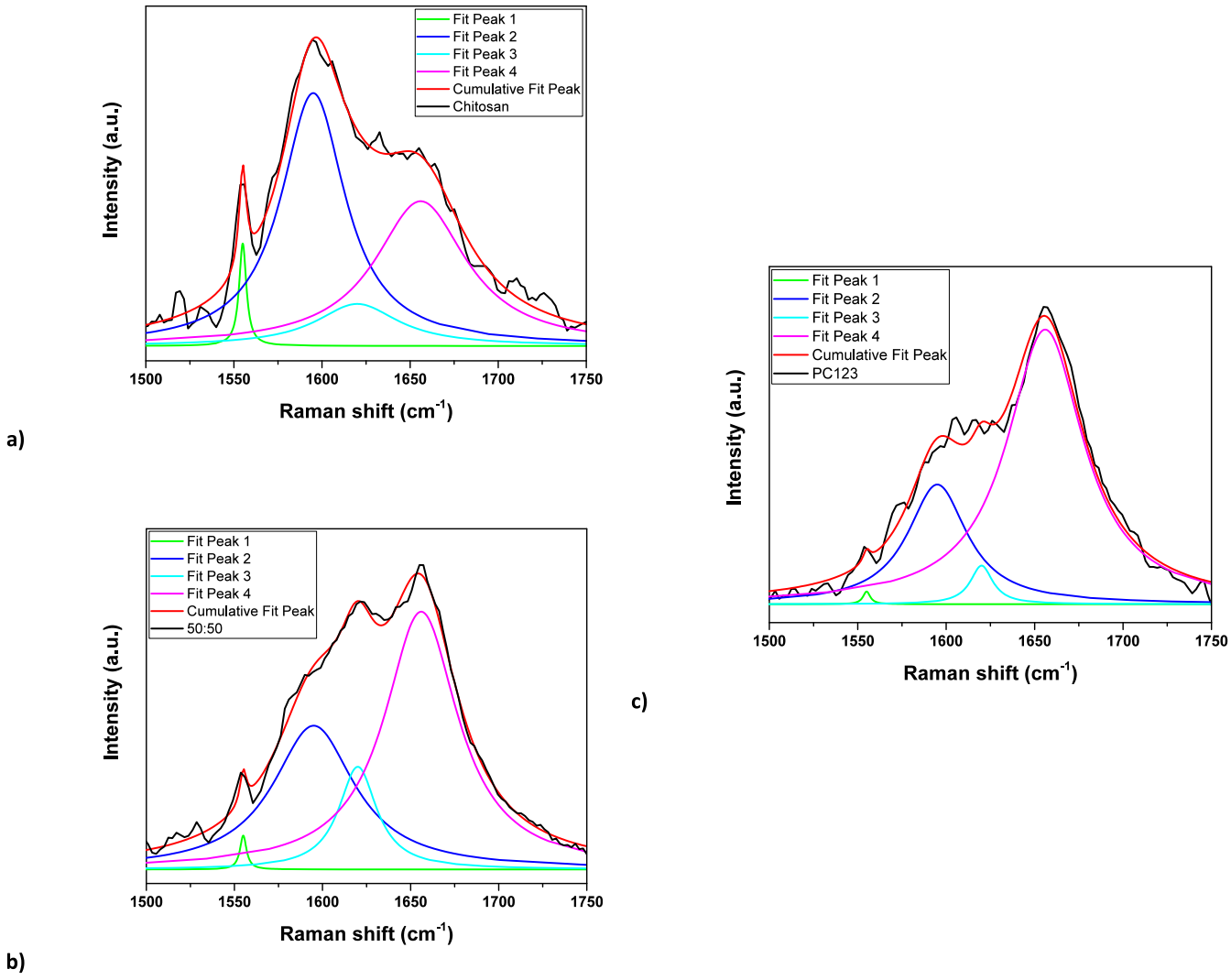

Fig. 4. Deconvolution of the Raman bands of pure chitosan (a), 50 wt% chitosan:50 wt% chitin (b), and PC123 (c) in the region of interest (1500–1750 cm^{-1}).

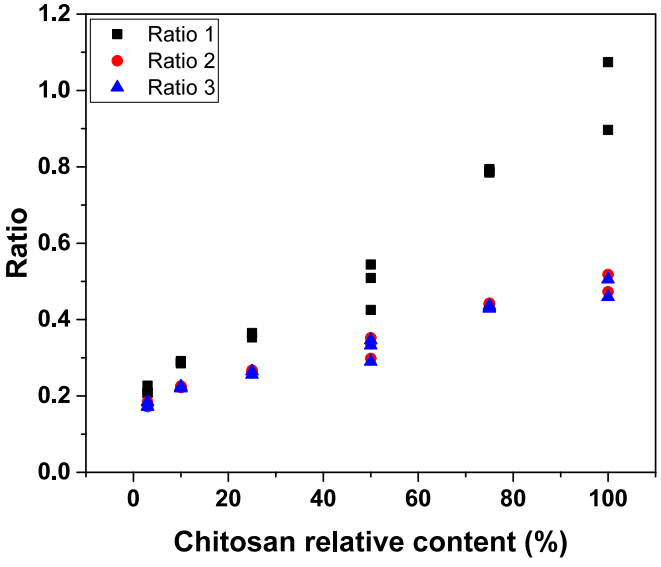

Fig. 5. Relationships among the three different ratios obtained from the integrated areas of the bands corresponding to the vibrational modes of chitosan and chitin and relative chitosan content of the samples.

Table 4
Linear fitting parameters (Chitosan relative content (%) = a + b•Ratio) for the calibration of the three tested ratios.

	Ratio 1	Ratio 2	Ratio 3
a	−20.38	−51.83	−53.60
b	123.10	296.78	307.43
R^2	0.958	0.974	0.971
SD (a)	15.61	17.21	18.70
LOD (%)	0.42	0.19	0.20

result suggests that this approach could be sensible down to very low chitosan relative contents. However, further improvement of the calibration with reference samples with chitosan relative contents below 3 % would be advisable to study samples within that range.

The above-described measurement and estimation procedures were performed on five fungal strain samples (Materials and Methods Section: Sample Preparation). Analysis of fungal samples was difficult due to the high background fluorescence of the fungal cell wall compounds other than chitin and chitosan. This resulted in low-quality spectra. Nevertheless, as no other signals were detected in the selected region, Raman spectral characteristic of chitin and chitosan were recorded (Fig. 4).

The obtained fungal spectra were deconvoluted, and the three ratios of integrated areas were calculated (Table 5). Then, the ratios were introduced into the calibration models to estimate the relative chitosan

Table 5
Observed ratios and estimated chitosan contents relative to the total chitosan and chitin content determined based on each ratio.

Fungal strain	Ratio 1	Chitosan estimation (wt%)	Ratio 2	Chitosan estimation (wt%)	Ratio 3	Chitosan estimation (wt%)
126KNY	0.322	19.3	0.243	20.3	0.238	19.6
85SCT	0.326	19.8	0.245	20.9	0.242	20.8
PC123	0.347	22.3	0.257	24.4	0.253	24.2
447ZAF	0.348	22.5	0.258	24.7	0.253	24.2
69NZ	0.360	23.9	0.270	28.3	0.263	27.3

content in each strain (Table 5).

Relative chitosan content was 19–28 wt% in the tested fungi. Relative chitosan and chitin contents were similar to those previously reported (Table 1). Notably, total amounts of chitin and chitosan (Table 2) did not affect the relative chitosan content determined via Raman spectroscopy (high amounts of chitin and chitosan did not indicate high chitosan content; Table 5). Moreover, the three proposed ratios preserved the relative chitosan content among the samples. However, slight differences were observed in the values indicated by each ratio, suggesting the need for additional investigation, including the validation of measured chitosan content of fungal samples with that determined by other techniques, to optimize the calibration for more accurate results. As a partial validation approach, an additional chitosan:chitin mixture was prepared and studied following this approach. The relative amount of chitosan for this mixture was fixed in 20 wt%, aiming to have a reference sample within the chitosan content range determined for the studied fungi. Table 6 shows the ratios and estimated chitosan content obtained from three measurements of this reference sample. Ratios 1 and 2 seem to be more accurate than ratio 3, providing average chitosan content estimations closer to the actual value (20 wt%). Moreover, the three ratios present similar standard deviations, around 1 wt%.

In addition to the previous results, our data provided a narrow range of chitosan content per mg DW by combining the acid hydrolysis and Raman spectroscopy results (Table 7).

We also compared the amounts of chitin and chitosan determined in this study with those reported in other species (Table 1). Lam and Diep reported significant inhibition of *Aspergillus nidulans* in the presence of chitosan in the medium [19]. *Aspergillus nidulans* exhibits 3.9 wt% chitosan/dry cell wall weight [20]. Ben-Shalom *et al.* reported the sensitivity of *Botrytis cinerea* to chitosan [21], which exhibits a relative content of 1.9 wt% chitosan/dry cell wall weight [20]. A clear difference in chitosan content relative to the dry mass of mycelia was observed between this study, with values of approximately 9–11 wt% (Table 6), and previous literature, except for *A. niger* that exhibits comparable values of approximately 11.0 wt% [31]. These findings indicate that chitosan-resistant fungi (see section 2.1), such as *P. chlamydosporia*, exhibit higher amounts of chitosan relative to the total mass of the sample than the chitosan-sensitive fungi, such as *Aspergillus nidulans* or *B. cinerea*. Therefore, it can be expected that fungi can deacetylate chitin in their cell wall to increase the chitosan ratio and protect their cell wall. However, results of previous studies were obtained using an extraction method with non-soluble materials at alkaline pH, which could be less sensitive than the Raman technique used in this study. Moreover, these reported approaches require complex multi-step procedures to determine the chitosan content, including lyophilization, grounding, mixing with NaOH solutions, homogenization, autoclaving, centrifugation, etc. [20]. On the contrary, the proposed approach using Raman spectroscopy only requires of the lyophilization and grounding. Nevertheless, future studies should compare both techniques in the same fungi to verify these findings.

Table 7
Obtained chitosan content per mg DW.

Fungi	Estimated chitosan content (mg/mg DW)		
126KNY	0.105	–	0.111
85SCT	0.097	–	0.102
PC123	0.096	–	0.105
447ZAF	0.089	–	0.098
69NZ	0.132	–	0.157

This study successfully estimated the relative contents of chitosan and chitin in the fungal cell wall using Raman spectroscopy. Our method discriminated among different fungal samples based on their relative chitosan content in combination with the standard technique, acid hydrolysis, that provided quantitative data on chitin and chitosan. Further improvement of our approach and use of systems to decrease fluorescence, such as Fourier-transform-Raman, could yield more advanced and precise techniques for the quantitative determination of the relative chitosan and chitin contents in fungi.

4. Conclusions

In conclusion, this study established an approach based on Raman spectroscopy to estimate the chitosan:chitin ratio in lyophilized fungal samples. Appropriate selection of the spectral region of interest without any interference of other components (1500–1750 cm^{-1}), along with the use of a reference dataset of chitosan:chitin blends, facilitated the study of fungal cell wall components. Initially, a linear trend was observed for the center of gravity of the bands in the 1540–1740 cm^{-1} range; however, it could not be explored further due to the resolution limitation of our experimental setup. Then, the obtained bands of chitosan:chitin blends in the 1540–1740 cm^{-1} range were deconvoluted by fitting them according to the dynamic vibrational Raman modes of chitosan and chitin, and three ratios were obtained from the integrated areas of the vibrational modes corresponding to both molecules, which were directly proportional to the relative chitosan contents. The developed method was successfully used to estimate the relative chitosan and chitin contents of five fungal strains, as well as of a reference sample with known chitosan content, obtaining just slight differences in the absolute values but consistent orders of magnitude and relative orders provided by each ratio. Moreover, combination of our method with acid hydrolysis provided an efficient approach to determine not only the total chitin and chitosan contents in the fungal cell wall, but also estimate the contents of each one of them. Overall, this study provides an approach to accurately determine the cell wall composition of fungi, providing key insights into the interactions between fungi and the environment.

CRediT authorship contribution statement

Suset Barroso-Solares: Writing – review & editing, Writing – original draft, Investigation. **Federico Lopez-Moya:** Writing – review &

Table 6
Observed ratios and estimated chitosan contents for the reference sample with 20.0 wt% relative chitosan content.

20:80 sample	Ratio 1	Chitosan estimation (wt%)	Ratio 2	Chitosan estimation (wt%)	Ratio 3	Chitosan estimation (wt%)
Measure 1	0.319	18.9	0.242	20.0	0.242	20.8
Measure 2	0.333	20.7	0.250	22.4	0.250	23.3
Measure 3	0.322	19.2	0.243	20.4	0.243	21.2
Average	0.325	19.6	0.245	20.9	0.245	21.8
SD	0.006	0.8	0.004	1.0	0.004	1.1

editing, Investigation. **Teresa Fraile:** Writing – review & editing, Writing – original draft, Investigation. **Ángel Carmelo Prieto:** Writing – review & editing, Methodology, Supervision, Funding acquisition. **Luis Lopez-Llorca:** Writing – review & editing, Methodology, Supervision, Funding acquisition. **Javier Pinto:** Writing – review & editing, Investigation, Methodology, Funding acquisition.

Funding

This work was supported by the Regional Government of Castilla y León and the EU-FEDER program (CLU-2019-04 and VA210P20), MCIN/AEI/10.13039/501100011033 and the EU NextGenerationEU/PRTR program (PLEC2021-007705), and project PID-2020-119734RB-I00 funded by the Spanish Ministry of Science and Innovation.

Declaration of competing interest

The authors declare the following financial interests/personal relationships which may be considered as potential competing interests: Javier Pinto reports financial support was provided by Regional Government of Castilla y León and the EU-FEDER program. Javier Pinto reports financial support was provided by MCIN, AEI and the EU NextGenerationEU PRTR program. Luis Lopez-Llorca reports financial support was provided by Spanish Ministry of Science and Innovation. If there are other authors, they declare that they have no known competing financial interests or personal relationships that could have appeared to influence the work reported in this paper.

Acknowledgements

We would like to thank Cristina Mingot-Ureta of the Plant Pathology Laboratory (Department of Marine Sciences and Applied Biology, University of Alicante, Spain) for technical support.

Data availability

Data will be made available on request.

References

[1] J. De Gelder, K. De Gussem, P. Vandenabeele, L. Moens, Reference database of Raman spectra of biological molecules, J. Raman Spectrosc. 38 (2007) 1133–1147, https://doi.org/10.1002/jrs.1734.
[2] M. Wysokowski, V.V. Bazhenov, M.V. Tsurkan, R. Galli, A.L. Stelling, H. Stöcker, S. Kaiser, E. Niederschlag, G. Gärtner, T. Behm, M. Ilan, A.Y. Petrenko, T. Jesionowski, H. Ehrlich, Isolation and identification of chitin in three-dimensional skeleton of Aplysina fistularis marine sponge, Int. J. Biol. Macromol. 62 (2013) 94–100, https://doi.org/10.1016/j.ijbiomac.2013.08.039.
[3] A. Kudelski, Analytical applications of Raman spectroscopy, Talanta 76 (2008) 1–8, https://doi.org/10.1016/j.talanta.2008.02.042.
[4] R.S. Das, Y.K. Agrawal, Raman spectroscopy: Recent advancements, techniques and applications, Vib. Spectrosc. 57 (2011) 163–176, https://doi.org/10.1016/j.vibspec.2011.08.003.
[5] E.S. Allakhverdiev, V.V. Khabatova, B.D. Kossalbayev, E.V. Zadneprovskaya, O. V. Rodnenkov, T.V. Martynyuk, G.V. Maksimov, S. Alwasel, T. Tomo, S. I. Allakhverdiev, Raman spectroscopy and its modifications applied to biological and medical research, Cells 11 (2022) 386, https://doi.org/10.3390/cells11030386.
[6] N.A.R. Gow, J.P. Latge, C.A. Munro, The fungal cell wall: structure, biosynthesis, and function, FUNK-0035-2016, Microbiol. Spectr. 5 (2017), https://doi.org/10.1128/microbiolspec.FUNK-0035-2016.
[7] H. Noothalapati, T. Sasaki, T. Kaino, M. Kawamukai, M. Ando, H.O. Hamaguchi, T. Yamamoto, Label-free chemical imaging of fungal spore walls by Raman microscopy and multivariate curve resolution analysis, Sci. Rep. 6 (2016) 1–10, https://doi.org/10.1038/srep27789.
[8] M. Kaya, M. Mujtaba, H. Ehrlich, A.M. Salaberria, T. Baran, C.T. Amemiya, R. Galli, L. Akyuz, I. Sargin, J. Labidi, On chemistry of γ-chitin, Carbohydr. Polym. 176 (2017) 177–186, https://doi.org/10.1016/j.carbpol.2017.08.076.
[9] A. Synytsya, M. Novak, Structural analysis of glucans, Ann. Transl. Med. 2 (2014) 1–14, https://doi.org/10.3978/j.issn.2305-5839.2014.02.07.
[10] S. Fischer, K. Schenzel, K. Fischer, W. Diepenbrock, Applications of FT Raman spectroscopy and micro spectroscopy characterizing cellulose and cellulosic biomaterials, Macromol. Symp. 223 (2005) 41–56, https://doi.org/10.1002/masy.200550503.
[11] A. Zając, J. Hanuza, M. Wandas, L. Dymińska, Determination of N-acetylation degree in chitosan using Raman spectroscopy, Spectrochim. Acta - Part A Mol. Biomol. Spectrosc. 134 (2015) 114–120, https://doi.org/10.1016/j.saa.2014.06.071.
[12] M.S. Mikkelsen, B.M. Jespersen, F.H. Larsen, A. Blennow, S.B. Engelsen, Molecular structure of large-scale extracted β-glucan from barley and oat: identification of a significantly changed block structure in a high β-glucan barley mutant, Food Chem. 136 (2013) 130–138, https://doi.org/10.1016/j.foodchem.2012.07.097.
[13] H.U. Rehman, S. Cord-Landwehr, V. Shapaval, S. Dzurendova, A. Kohler, B. M. Moerschbacher, B. Zimmermann, High-throughput vibrational spectroscopy methods for determination of degree of acetylation for chitin and chitosan, Carbohydr. Polym. 302 (2023) 120428, https://doi.org/10.1016/j.carbpol.2022.120428.
[14] M.V. Tsurkan, A. Voronkina, Y. Khrunyk, M. Wysokowski, I. Petrenko, H. Ehrlich, Progress in chitin analytics, Carbohydr. Polym. 252 (2021) 117204, https://doi.org/10.1016/j.carbpol.2020.117204.
[15] H.E. Brown, S.K. Esher, J.A. Alspaugh, Chitin: A "Hidden Figure" in the fungal cell wall, in: J. Latgé (Ed.), Fungal Cell Wall. Curr. Top. Microbiol. Immunol., 2019: pp. 83–111. Doi: 10.3109/08820137709055812.
[16] N.E. El Gueddari, U. Rauchhaus, B.M. Moerschbacher, H.B. Deising, Developmentally regulated conversion of surface-exposed chitin to chitosan in cell walls of plant pathogenic fungi, New Phytol. 156 (2022) 103–112.
[17] F. Lopez-moya, M. Suarez-fernandez, L.V. Lopez-llorca, Molecular mechanisms of chitosan interactions with fungi and plants, Int. J. Mol. Sci. 20 (2019) 332, https://doi.org/10.3390/ijms20020332.
[18] T. Wu, S. Zivanovic, F.A. Draughon, C.E. Sams, Chitin and chitosan-value-added products from mushroom waste, J. Agric. Food Chem. 52 (2004) 7905–7910, https://doi.org/10.1021/jf0492565.
[19] N. Duy Lam, T. Bang Diep, A preliminary study on radiation treatment of chitosan for enhancement of antifungal activity tested on fruit-spoiling strains, Nucl. Sci. Technol. 2 (2003) 54–60.
[20] K.J. Hu, J.L. Hu, K.P. Ho, K.W. Yeung, Screening of fungi for chitosan producers, and copper adsorption capacity of fungal chitosan and chitosanaceous materials, Carbohydr. Polym. 58 (2004) 45–52, https://doi.org/10.1016/j.carbpol.2004.06.015.
[21] N. Ben-Shalom, R. Ardi, R. Pinto, C. Aki, E. Fallik, Controlling gray mould caused by Botrytis cinerea in cucumber plants by means of chitosan, Crop Prot. 22 (2003) 285–290, https://doi.org/10.1016/S0261-2194(02)00149-7.
[22] T.S.A. Monteiro, E.A. Lopes, H.C. Evans, Perspectives in sustainable nematode management through Pochonia chlamydosporia applications for root and rhizosphere health, in: R.H. Manzanilla-López, L.V. Lopez-Llorca (Eds.), Sustain. Plant Crop Prot., Springer International Publishing AG, 2017: pp. 77–96. Doi: 10.1007/978-3-319-59224-4.
[23] R.H. Manzanilla-López, I. Esteves, M.M. Finetti-Sialer, P.R. Hirsch, E. Ward, J. Devonshire, L. Hidalgo-Díaz, Pochonia chlamydosporia: advances and challenges to improve its performance as a biological control agent of sedentary endo-parasitic nematodes, J. Nematol. 45 (2013) 1–7.
[24] R. Nicoletti, A. Becchimanzi, Endophytism of lecanicillium and akanthomyces, Agriculture 10 (2020) 1–16, https://doi.org/10.3390/agriculture10060205.
[25] S.L. Jat, S.B. Suby, C.M. Parihar, G. Gambhir, N. Kumar, S. Rakshit, Microbiome for sustainable agriculture: a review with special reference to the corn production system, Arch. Microbiol. 203 (2021) 2771–2793, https://doi.org/10.1007/s00203-021-02320-8.
[26] C.M. Olivares-Bernabeu, L.V. López-Llorca, Fungal egg-parasites of plant-parasitic nematodes from Spanish soils, Rev. Iberoam. Micol. 19 (2002) 104–110.
[27] T. Pusztahelyi, Chitin and chitin-related compounds in plant–fungal interactions, Mycology 9 (2018) 189–201, https://doi.org/10.1080/21501203.2018.1473299.
[28] E. Oliveira-garcia, H.B. Deising, Infection structure – specific expression of b-1,3-glucan synthase is essential for pathogenicity of Colletotrichum graminicola and evasion of b-Glucan – triggered immunity in maize, Plant Cell 25 (2013) 2356–2378, https://doi.org/10.1105/tpc.112.103499.
[29] A. Aranda-Martinez, F. Lopez-Moya, L.V. Lopez-Llorca, Cell wall composition plays a key role on sensitivity of filamentous fungi to chitosan, J. Basic Microbiol. 56 (2016) 1059–1070, https://doi.org/10.1002/jobm.201500775.
[30] K. Xing, X. Shen, X. Zhu, X. Ju, X. Miao, J. Tian, Z. Feng, X. Peng, J. Jiang, S. Qin, Synthesis and in vitro antifungal efficacy of oleoyl-chitosan nanoparticles against plant pathogenic fungi, Int. J. Biol. Macromol. 82 (2016) 830–836, https://doi.org/10.1016/j.ijbiomac.2015.09.074.
[31] P. Pochanavanich, W. Suntornsuk, Fungal chitosan production and its characterization, Lett. Appl. Microbiol. 35 (2002) 17–21.
[32] T. Tianwei, W. Binwu, S. Xinyuan, Separation of chitosan from Penicillium chrysogenum mycelium and its applications, J. Bioact. Compat. Polym. 17 (2002) 173–182, https://doi.org/10.1106/088391102026103.
[33] H. Ehrlich, M. Maldonado, K.D. Spindler, C. Eckert, T. Hanke, R. Born, C. Goebel, P. Simon, S. Heinemann, H. Worch, First evidence of chitin as a component of the skeletal fibers of marine sponges. Part I. Verongidae (Demospongia: Porifera), J. Exp. Zool. Part B Mol. Dev. Evol. 308 (2007) 347–356. Doi: 10.1002/jez.b.21156.